J Mol Model (2007) 13:751–756
DOI 10.1007/s00894-007-0218-3

ORIGINAL PAPER

Development of realistic models for Double Metal Cyanide catalyst active sites

Jacek C. Wojdeł · Stefan T. Bromley · Francesc Illas · Jacobus C. Jansen

Received: 15 November 2006 / Accepted: 30 April 2007 / Published online: 13 June 2007

Abstract Realistic molecular models of one and two-centre catalytic active sites originating from the cleavage of a precursor material known to give rise to an active double metal cyanide catalyst are described. Via periodic density functional calculations the structure of the proposed catalytic sites are shown to be dependent on electrostatic and structural relaxation processes occurring at the surfaces of the precursor material. It is shown how these effects may be adequately captured by small molecular models of the active sites. The general methodology proposed should provide a computationally efficient basis for detailed future studies into catalytic reactions over double metal cyanide materials.

Keywords DFT modelling · Double metal cyanide catalyst · Heterogenous catalysis

This work has been originally presented on the Modelling and Design of Molecular Materials conference in Wrocław, Poland.

J. C. Wojdeł · S. T. Bromley (✉) · F. Illas
Department de Química Física & Centre Especial de Recerca en Química Teòrica,
Universitat de Barcelona & Parc Científic de Barcelona,
C/Martí i Franquès 1,
08028 Barcelona, Spain
e-mail: S.Bromley@qf.ub.es

J. C. Jansen
Ceramic Membrane Centre "The Pore", DelftChemTech,
Delft University of Technology,
Julianalaan 136,
2628BL Delft, The Netherlands

Introduction

Double Metal Cyanide (DMC) catalysts are a class of molecular salts comprising of a metal-cyanide crystalline framework with two different metal centres and a general formula $M^1_x[M^2(CN)_6]_y$ ($M^1 = Zn$, $M^2 = Co$, Fe) [1–4]. In recent years DMC catalysts have become industrially important for epoxide polymerisation of polyols. Their main advantages over more traditional potassium base (KOH) catalyst are (i) a much higher activity, (ii) highly reduced unsaturation of the obtained polyols, and (iii) a narrow molecular weight distribution of the product [5, 6]. The above features result in the possibility of reaching much higher polyol molecular weights than using a KOH catalyst in a more controlled manner. The polyols prepared in such a process are useful in the production of polyurethane coatings, elastomers, sealants, foams and adhesives [7]. In the light of growing environmental concerns, the DMC catalyst has also been proposed as an agent for co-polymerising carbon dioxide with epoxides, enabling the environmentally unfriendly properties of CO_2 to be suppressed by using it as a raw material source for polymer production [8]. DMC catalysts are also found to be active in copolymerisation of other molecular species [9].

DMC catalysts have been relatively well investigated with respect to their activity in different preparation routes and operating conditions [2, 4, 5, 10]. However, we are not aware of any theoretical investigation into the exact mechanism of the DMC mediated catalysis to date, nor the detailed nature of the active sites. In the present study, we start with the crystal structure of the DMC precursor salt, which has been obtained from refined powder diffraction data. The DMC bulk is then constructed by the substitution of hydroxyl groups with chloride anions. The resulting structure is then optimised using fully periodic

density functional (DF) calculations and planewave pseudopotentials, both with respect to lattice parameters and atomic positions. Finally, the slab model is used to calculate a reconstructed surface of the DMC catalyst from which we extract likely active site models.

Periodic and slab calculations

The aim of the present investigation is to select a small atomic cluster with which to adequately represent the active site of the DMC catalyst. The model system must be small enough so that the calculations of full catalytic cycle are feasible, but at the same time, it must represent the active site with appropriate accuracy under a range of conditions (i.e. empty site, site with Cl^- on top, site with adsorbed reactants). As the DMC material is ionic, an important consideration is the role of the long range electrostatics of the material on the localised active site. We have investigated these long range effects using fully periodic DFT calculations on bulk crystal, and surface slab models. For this type of calculation we used the pseudopotential planewave (PP-PW) approach with Vanderbilt ultrasoft pseudopotentials (USPPs) [11]. In all calculations, we used the PW91 exchange and correlation functional [12], and the calculations were done at Γ point. No *k*-point sampling was deemed necessary in our calculations for two reasons: we are using a relatively large unit cell (at least 7Å in each direction), and the fact that the DMC is an insulating ionic salt. It is worth noting that interesting surface properties were calculated using even larger 2×2 super-cell, further reducing the need for *k*-point sampling.

Two different codes were used in the calculations. For the fully periodic calculations, we used CPMD code from IBM research labs [13]. Because of the fact that CPMD does not allow for calculation of the stress tensor with USPPs, unit cell optimisation was achieved by sampling the total energy landscape for different cell parameters, and finding the minimum of a quadratic best fit. Within each set of unit cell parameters, full geometry optimisation was done at a planewave kinetic energy cut-off of 500 eV. In order to minimise the effects of Pulay stress, the final energies were obtained by taking the optimised geometry and performing a single step energy calculation at a 1000 eV cut-off.

In calculations of the surface reconstruction of the DMC catalyst, we used the Dacapo code from the Campos Atomistic Simulation Environment [14]. For these calculations we used 300 eV energy cutoff, which proved to be sufficient for both energy and geometry convergence. In all calculations, we used a super-cell containing a slab thick enough to contain two layers of $Co(CN)_6^{3-}$ complexes, and four layers of Zn^{2+} centres. The super-cell extended to 2×2 unit cells parallel to the surface. After cutting the slab out of the crystal, the super-cell was augmented with 10Å of empty space perpendicular to the crystal surface.

Due to the asymmetric distribution of surface terminating anions (Cl^-, or OH^-) after a simple cleavage of the crystal (along the [100] plane to reveal the Zn centres) an unphysically high dipole moment acts on the interior of the slab. Potential mechanisms for dipole quenching in ionic materials such as the DMC precursor have been postulated by Tasker [15] and recently reviewed by Noguera [16]. The key to all these mechanisms is a removal, or compensation, of the excess surface charge, which can be accomplished by ionic reconstruction, electron transfer between the two surfaces, or adsorption of charged moieties, e.g. in an electrolyte. In order to counteract the dipole build up our system the terminating anions were distributed evenly on both surfaces of the DMC crystal. We argue that the maintenance of this fractional anion occupancy (e.g. during crystal growth or cleavage) is a natural physical/chemical mechanism by which DMC crystallites adopt to avoid the energetic cost of the accumulation of an dipole.

In test calculations employing full optimisation of smaller slabs, changes in the geometry of the crystal were only significant at the surfaces due to reconstruction but were found to be negligible below the first surface layer of zinc centres. The high stability of the bulk is due to the rigidity of hexacyanide complexes which keep the internal part of the crystal firmly fixed. In order to reduce the computational cost of the final large slab calculations, the positions of inner atoms of the slab were fixed and only the positions of terminating anions, zinc centres and first layer of cyanide groups were optimised.

Molecular calculations

For all of the molecular calculations we used cluster DF calculations with the B3LYP hybrid exchange correlation functional [17] and an effective core potential basis set (LANL2DZ) [18]. The calculations were done using two codes: Gaussian98 [19] and GAMESS-UK [20]. We decided to use a different density functional for the cluster calculations than for periodic ones, because of its superior performance to non-hybrid functionals in many calculations of catalysed reactions. Unfortunately this functional was not available in the periodic codes we used. In all cases the calculated geometries and electronic properties of the catalytic centre in both cluster and periodic calculations were checked for consistency between the two employed functionals.

For cluster calculations on single-and double-centre sites, the geometry of the cluster was partially fixed to reflect the rigidity of the surface. The initial geometries

of these clusters were taken from the periodic surface relaxation calculations and cut after the first layer of cyanide groups. The resulting geometries used in the cluster calculations are presented in Fig. 1. It is important to note, that such clusters are charged, and geometrically stressed. Without additional treatment, obtaining a self-consistent solution of their electronic structure is extremely difficult. In order to counteract this problem, the clusters were additionally terminated with point charges to simulate the electrostatic influence of the rest of the crystal (therefore decreasing both geometrical and electronic stress). The point charges were placed at the centres of where the $Co(CN)_6$ complexes reside in the bulk crystal. During the calculations the positions of all zinc and chloride atoms were optimised. Using two different codes for the calculations both in the molecular and periodic case, was primarily motivated by the availability and efficiency of the codes on different computing facilities used in the course of this study. Some calculations were repeated in order to verify the transferability of the results.

Crystal structure of the DMC precursor and catalyst

In the experiment the DMC catalyst is prepared using a process described first by Kuyper and Boxhorn [1]. In this procedure, the catalyst goes through an intermediate form, which can be crystallised and for which the structure has been resolved. The (unpublished as of yet) structure has been refined by J.B. van Mechelen and co-workers in the Laboratory for Crystallography, University of Amsterdam. We obtained the details of the structure in private correspondence from Shell Chemicals, and used it to set up the calculations.

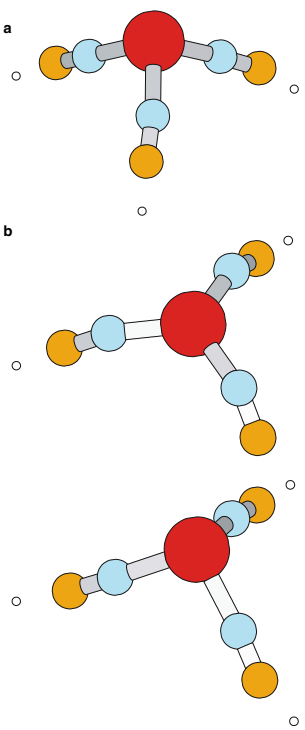

Fig. 1 Catalytic centre geometries used in cluster calculations: (**a**) single centre and (**b**) double centre

The originally refined crystal structure of DMC precursor has a relatively large unit cell, comprising of six $Co(CN)_6$ ions and 12 zinc atoms. This size of the unit cell puts significant computational strain on the possibility of modelling the crystal structure in a fully periodic manner. However, thanks to the near symmetrical arrangement of the atoms within the unit cell, it can be simplified to a cell which is three times smaller. The resulting structure fits the original refined one within a 0.05Å margin. All of the further described periodic DF calculations refer to this simplified unit cell. The calculated crystal structure of the DMC precursor is listed in Table 1.

Surface reconstruction on the DMC catalyst

The DMC material is a heterogeneous catalyst, with catalysis happening in a slurry of DMC, propylene oxide and polyol starters. Looking at the crystal structure, the [100] surface appears to be the best candidate for the active part of the catalyst due to the fact that: (i) this surface is easily formed by cleaving just one bond per unit cell, and (ii) the surface exposes a layer of regularly spaced Zn centres. In our extended 2×2×1 super-cell, we placed two Cl^- anions on each side of the slab, which ensures quenching of the electrostatic dipole across the slab (see Fig. 2). It can be argued that in a real surface, this distribution might be somewhat more complex, but we believe that because of high rigidity of $Co(CN)_6$ anion, and the relatively long distance between Zn centres (7.5Å) it will not substantially influence the properties of the active site.

In the periodic DF calculations, the surface undergoes a slight reconstruction, which is found to influence only the topmost layer of the zinc centres. The Zn centres which are not occupied by Cl^- anions sink inside the slab, and eventually become almost co-planar with the nitrogen atoms. The displacement of the Zn centres from the N-plane is found to be 0.23Å. On the other hand, the Zn centres having corresponding Cl^- anions protrude out of the surface, with the Cl-Zn bond almost perpendicular to the surface plane (compared to a 48° angle between the corresponding bond and the [100] plane inside bulk of the crystal).

We find therefore that the geometry of the surface around the Zn centres is heavily influenced by the availability of anions to be attached to it. This structural change leads also to significant changes in electronic properties of the zinc centres. We can quantify these

Table 1 Calculated atomic coordinates of the DMC catalyst, and its precursor

	DMC precursor				DMC bulk		
a/b/c	7.40	7.40	16.53	a/b/c	7.51	7.51	17.35
$\alpha/\beta/\gamma$	90.0	90.0	120.0	$\alpha/\beta/\gamma$	90.0	90.0	120.0
spacegroup	$P_{11\,m}$			spacegroup	$P_{11\,m}$		
H	0.918	0.581	0.0				
H	0.724	0.772	0.5				
O	0.068	0.641	0.0	Cl	0.049	0.542	0.0
O	0.784	0.922	0.5	Cl	0.710	0.792	0.5
C	0.358	0.440	0.184	C	0.364	0.465	0.216
C	0.232	0.214	0.310	C	0.234	0.177	0.346
C	0.585	0.568	0.307	C	0.549	0.568	0.346
C	0.360	0.088	0.190	C	0.329	0.088	0.215
C	0.712	0.442	0.193	C	0.705	0.429	0.216
C	0.586	0.215	0.317	C	0.625	0.253	0.346
N	0.284	0.520	0.145	N	0.284	0.541	0.183
N	0.075	0.142	0.346	N	0.088	0.102	0.386
N	0.288	0.931	0.154	N	0.252	0.918	0.181
N	0.663	0.731	0.339	N	0.621	0.715	0.385
N	0.874	0.522	0.160	N	0.862	0.510	0.183
N	0.666	0.143	0.356	N	0.700	0.181	0.386
Zn	0.143	0.659	0.112	Zn	0.179	0.656	0.108
Zn	0.803	0.999	0.388	Zn	0.792	0.029	0.393
Co	0.471	0.326	0.250	Co	0.469	0.332	0.281

changes by performing Bader analysis [21] of the charge density, and examining the resulting atomic charges within the DMC slab (Table 2). As can be seen, in the absence of crystal induced electrostatic shielding, the Cl^- anion adopts a slightly higher negative charge on the surface than the inside bulk of the crystal. This charge comes at expense of the neighbouring unoccupied Zn centre, which becomes more positively charged. This in turn increases the polarisation of the attached CN ligands. The charges of the Zn centres and ligands directly underneath the Cl^- anions remain virtually unchanged from their bulk counterparts.

Molecular cluster model for active site

Our final model system for the active site, based on the calculated surface structure, has been verified with respect to the geometrical features found in periodic studies. We find that a model containing full layer of sub-surface ions (i.e. containing two Zn centres, and $Co(CN)_6$ anions connected to them) is capable of reproducing accurately the geometry of the surface Zn site after constrained relaxation. This model is, however, computationally very expensive, containing a total of five complex anions.

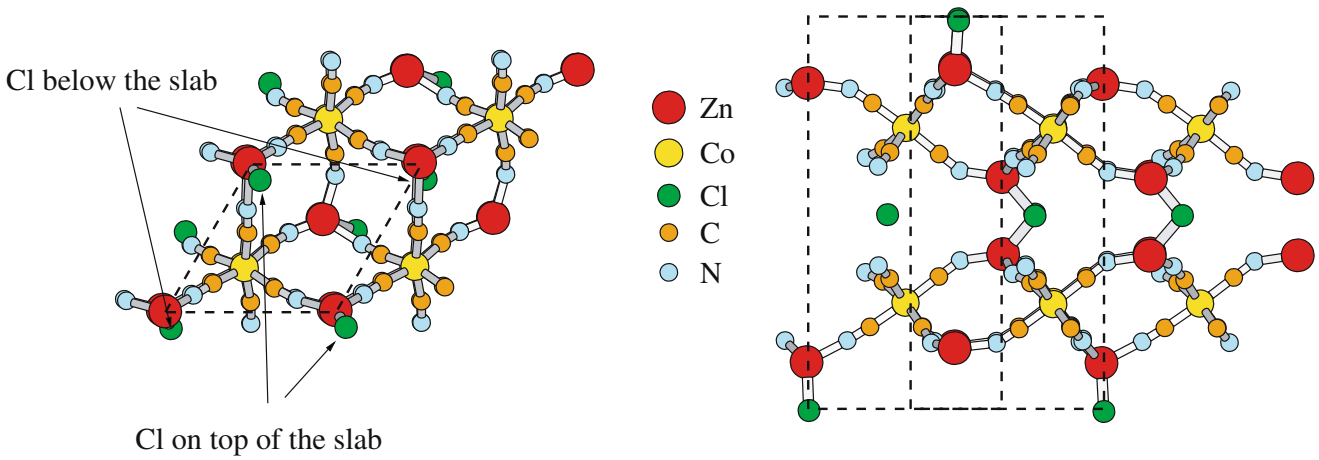

Fig. 2 Periodic slab model used for assessing surface reconstruction

Simply leaving out all complex anions, and terminating the CN ligands with hydrogen atoms does not yield a system with a proper relaxed surface site geometry. However, because of the rigidity of the hexacyanide anions and electronic shielding provided by cyanide ligands, we find that it is sufficient to substitute the first layer of $Co(CN)_6$ with fixed point charges, to reproduce the periodic active site geometry to within 0.05Å, for both empty and Cl^- occupied sites. This is an agreement found to hold even though different methodologies and different functionals are used in the respective cluster and periodic calculations (see Table 3). In optimising the cluster model the point charges and cyanide ligands are kept fixed while the Zn atoms and (possibly) Cl are allowed to relax. Several test runs with fixed/flexible N atoms yielded essentially equivalent geometries. The reported geometries for the double centre cluster reflect actually two spatially different parts of the same cluster, as it has been calculated with single Cl^- occupancy. In order to obtain single centre results, two calculations were done: (i) Cl^- occupied and (ii) empty site. In each case the number of electrons in the calculation was kept consistent with the formal charges of the involved atoms.

It is important to note, that in the cluster, while the point charges are placed where Co atom should reside in the crystal, each charge represents an approximation to each whole complex anion. The charge employed is therefore much less positive than the formal +3 charge on Co atom. We find, however, that the geometry of the site is not significantly influenced by the amount of charge placed, as it is effectively screened by the CN ligands. We tested charges in the range of 0.5 to 0.8, and eventually settled for 0.667 and 0.6 for the single centre cluster (three point charges) and double centre cluster (five point charges), respectively. These values made the whole molecular system charge neutral and was found to be optimal with respect to the rate of calculation convergence.

Table 2 Bader charges in the DMC slab model, and in the small molecular cluster

	Periodic calculation			
	Inside	Surface/Cl	Surface/empty	Cluster/Cl
Cl	−0.526	−0.622	–	−0.615
C	1.932	1.917	2.006	2.125
N	−2.456	−2.452	−2.521	−2.596
Co	1.209	–	–	−0.405
Zn	1.237	1.245	1.320	1.244

Note that in the case of the molecular cluster, the entry in the Co row represents the charge 'leakage' towards the point charges, which were considered valid centres in the Bader analysis.

Table 3 Comparison of calculated relevant bond distances (Å) and angles (degrees) of the active site

	Periodic	Single centre	Double centre
Zn^1-N	1.871	1.880	1.861
Zn^2-N	2.038	2.036	1.989
Zn^2-Cl	2.152	2.216	2.220
Zn^1-N-C	154.2	155.1	155.8
Zn^2-N-C	172.6	172.6	172.4

Zinc centres are numbered depending on Cl^- occupancy: (1) for free site, and (2) for occupied site.

Beside the good representation of structural properties of the site in cluster calculations, we also studied its electronic properties in the Cl^- occupied state; a configuration which will be relevant to further catalysis related calculations with Cl^- substituted by a deprotonised alcohol. Because of the fact that our model system is negatively charged when occupied by a Cl^- anion (2e for single centre model, and 3e for double centre model), there is a chance of electron leakage towards positive point charges. An analysis of charge distribution shows this indeed to be the case (see Table 2), but it also shows that the most charge is lost on the carbon side of highly polarisable CN^- ligand. The charges on Zn and Cl centres are only sightly affected, and their difference should not be given much significance because of the different calculation methodologies used. The charge densities of both periodic and cluster sites can be seen in Fig. 3.

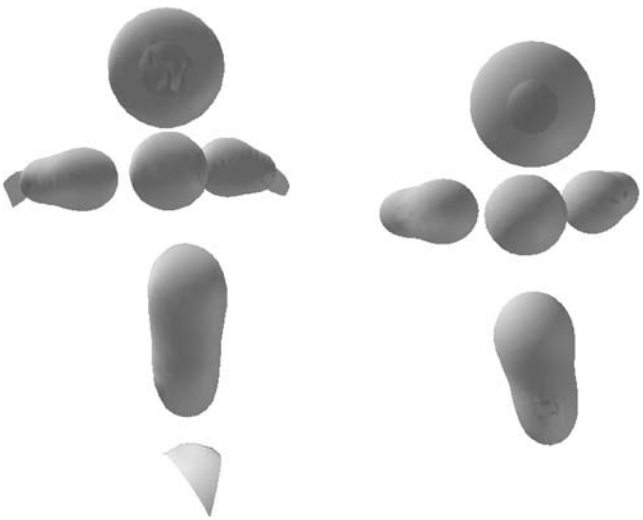

Fig. 3 Charge densities of the Cl occupied sites in the periodic (left) and cluster (right) calculations

Conclusions

In this paper, we demonstrate a systematic way of developing a computationally effective model for the active sites of a DMC catalyst. Starting from state of the art periodic calculations of the DMC catalyst precursor bulk, we obtained a model of the reconstructed DMC surface. The obtained surface model is then reduced to a small atomic cluster which represents the catalytic centre. In order to be able to investigate the possibility of bi-metallic activation, we present two different catalytic site models, containing one and two zinc centres. Our calculations show that both models are sufficient for capturing changes in the geometry of the modelled site depending on its Cl^- occupancy. Further results of calculations on the catalytic cycle employing these active site models will be presented elsewhere.

Acknowledgements This research has been financed by Shell Chemicals, Amsterdam as a part of "Application of Molecular Modeling to Catalysis Development" project.

References

1. Kuyper J, Boxhoorn GJ (1987) Catal 105:163–174
2. Huang YJ, Qi GR, Chen LS (2003) Appl Catal A 240:263–271
3. Chen S, Xu N, Shi J (2004) Prog Org Coat 49:125–129
4. Kim I, Ahn J-T, Lee S-H, Ha C-S, Park D-W (2004) Catal Today 93–95:511–516
5. O'Connor JM, Lickei DL (2000) Polyols derived from Double Metal Cyanide catalysts. In Proceedings of UTECH 2000, pp 6/1–6/9, The Hague, Rapra Conference Proceedings, 2000
6. Kim I, Ahn J-T, Park D-W, Lee S-H, Park I (2003) Stud Surf Sci Catal 145:529–530
7. Le-Khac B (2000) Arco Chemical Technology, LP US Patent 6,018,017
8. Kim I, Yi MJ, Byun SH, Park DW, Kim BU, Ha CS (2005) Macromol Symp 224:181–192
9. Hua Z, Qi G, Chen S (2004) J Appl Polym Sci 93:1788–1792
10. Kim I, Ahn J-T, Ha CS, Yang CS, Park I (2003) Polymer 44:3417–3428
11. Vanderbilt D (1990) Phys Rev B 41:7892–7895
12. Perdew JP, Chevary JA, Vosko SH, Jackson KA, Pederson MR, Singh DJ, Fiolhais C (1992) Phys Rev B 46:6671–6687
13. CPMD, Copyright IBM Corp 1990–2004, Copyright MPI für Festkörperforschung Stuttgart 1997–2001
14. CAMP open software project, http://www.fysik.dtu.dk/CAMPOS/
15. Tasker PW (1979) J Phys C 12:4977–4984
16. Noguera C (2000) J Phys-Condens Mat 12:R367–R410
17. Becke AD (1993) J Chem Phys 98:5648–5652
18. Hay PJ, Wadt WR (1985) J Chem Phys 82:270–283
19. Frisch MJ, Trucks GW, Schlegel HB, Scuseria GE, Robb MA, Cheeseman JR, Zakrzewski VG, Montgomery JA, Stratman RE, Burant JC, Dapprich S, Millam JM, Daniels AD, Kudin KN, Strain MC, Farkas O, Tomasi J, Barone V, Cossi M, Cammi R, Mennucci B, Pomelli C, Adamo C, Clifford S, Ochterski J, Petersson GA, Ayala PY, Cui Q, Morokuma K, Malick DK, Rabuck AD, Raghavachari K, Foresman JB, Cioslowski J, Ortiz JV, Baboul AG, Stefanov BB, Liu C, Liashenko A, Piskorz P, Komaromi, I, Gomperts R, Martin RL, Fox DJ, Keith T, Al-Laham MA, Peng CY, Nanayakkara A, Gonzalez C, Challacombe M, Gill PMW, Johnson BG, Chen W, Wong MW, Andres JL, Gonzales C, Head-Gordon M, Replogle ES, Pople JA (1998) Gaussian 98. Gaussian Inc, Pittsburgh PA
20. Guest M, Bush IJ, van Dam H, Sherwood P, Thomas J, van Lenthe J, Havenith R, Kendrick J (2005) Mol Phys 103:719–747
21. Bader RFW, Beddall PM, Cade PE (1971) J Am Chem Soc 93:3095–3107